Pyrometallurgical Reduction of Copper Slag with Biochar for Metal Recovery

Desmond Attah-Kyei[1] · Dmitry Sukhomlinov[1] · Lassi Klemettinen[1] · Radoslaw Michallik[2] · Hugh O'Brien[2] · Pekka Taskinen[1] · Daniel Lindberg[1]

Abstract

Large amounts of slag are generated during pyrometallurgical processing in copper production. Due to the presence of valuable elements, the improper disposal of huge quantities of copper slag produced, results in significant loss of resources as well as environmental issues. Analyses of the copper slag show that it contains valuable metals, particularly copper and nickel. In this work, four biochars were employed as fossil-free reducing agents to recover valuable metals from the slag. Reduction experiments were performed in a vertical furnace at temperatures 1250, 1300 and 1350 °C for 60 min in order to investigate the effect of temperature. Moreover, the effect of time on reduction progress was studied at 1250 °C and the concentrations of CO and CO_2 in the off-gas were measured with a gas analyzer. Copper slag was reacted with metallurgical coke for comparison and the products were analyzed with EPMA and LA-ICPMS. The results revealed that reduction rapidly progresses to the formation of metal alloy within 10 min. Valuable metals like copper, nickel and arsenic were the first to be reduced to the metal phase. As reduction time increased, iron was also reduced and combined with the metal droplet. The use of biochar as reductant was shown to be more effective than coke especially at lower temperatures. In addition, thermodynamic modelling was performed with FactSage and HSC and compared with the experimental results. The simulations with HSC showed the sequence of reactions taking place and the calculations by FactSage were in agreement with the experiments.

✉ Desmond Attah-Kyei
   desmond.attah-kyei@aalto.fi

   Dmitry Sukhomlinov
   dmitry.sukhomlinov@aalto.fi

   Lassi Klemettinen
   lassi.klemettinen@aalto.fi

   Radoslaw Michallik
   radoslaw.michallik@gtk.fi
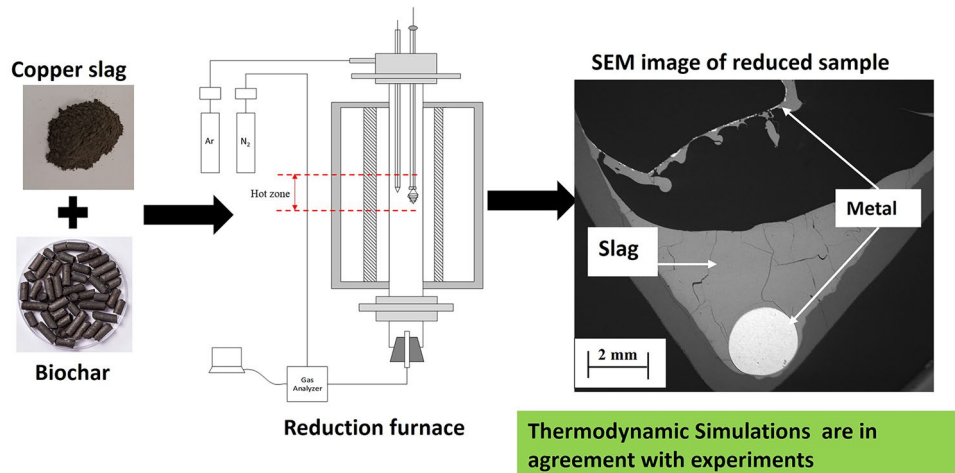
   Hugh O'Brien
   hugh.obrien@gtk.fi

   Pekka Taskinen
   pekka.taskinen@aalto.fi

   Daniel Lindberg
   daniel.k.lindberg@aalto.fi

1   Department of Chemical and Metallurgical Engineering, School of Chemical Engineering, Aalto University, Kemistintie 1, P.O. Box 16100, 00076 Aalto, Finland

2   Geological Survey of Finland, Vuorimiehentie 2, 02150 Espoo, Finland

Graphical Abstract

Introduction

Copper slag is generated as an unavoidable byproduct during pyrometallurgical processing of copper production. The total worldwide mine production of copper has risen in the past decade, increasing from 16 Mt in 2010 to 22 Mt in 2022 [1]. It is reported that for every ton of copper produced, 2.2–3 tons of slag is generated [2, 3]. Copper slag from industrial smelting usually contains 25–35 wt% silica, 1 wt% copper, 40 wt% iron as well as varying concentrations of Al_2O_3, CaO, and MgO. Minor amounts of elements such as Zn, As and Pb are present as well. Inappropriate disposal of copper slag causes environmental pollution due to the presence of hazardous elements. Despite its hazardous nature, copper slag possesses certain properties, such as high stability and abrasion resistance, which may be exploited in the manufacturing of cement, abrasive tools, asphalt concrete, cutting tools, glasses, and others [4–6]. The drawback of employing copper slags and other slags as construction material, e.g., in civil engineering, include the leachability of their minor elements, like zinc, arsenic and antimony, which are present as chemically dissolved oxides or within tiny mechanically entrapped sulfide matte or metal particles [7–9].

Copper slag also contains valuable elements and extensive studies aimed at recycling and reusing copper slags have been conducted. These include physical, hydrometallurgical, and pyrometallurgical separation methods either individually or in their combination, to recover valuable elements and help reduce impact on the environment [10, 11]. The techniques include froth flotation [12–14], leaching of valuable elements [15–17], roasting followed by flotation [18, 19] as well as magnetic separation [20–22]. Other studies conducted on carbothermic reduction of copper slag have investigated the recovery of valuable elements by pyrometallurgical processing [3, 20, 23, 24]. Carbothermic reduction typically employs coal, coke, diesel or natural gas as reductants. However, as energy shortages and environmental pollution intensify, the metallurgical industry needs
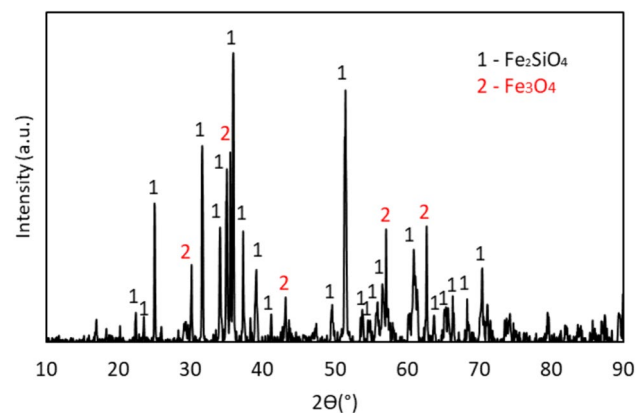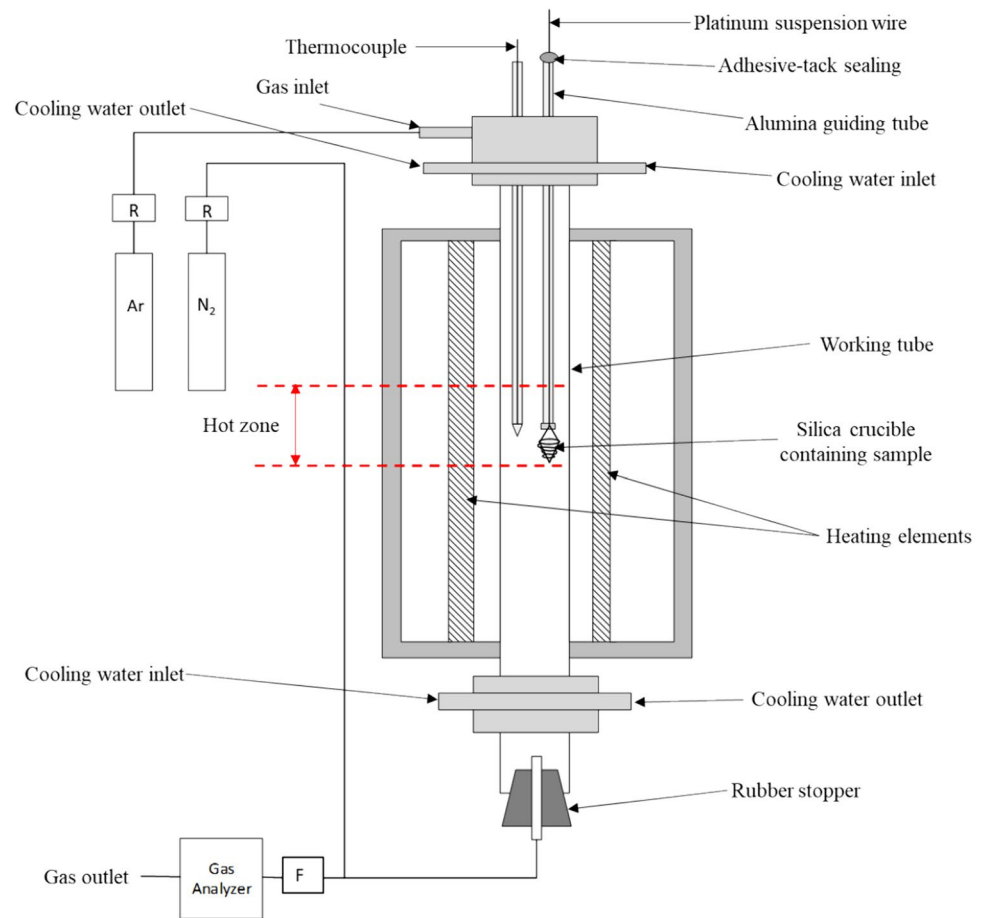

Fig. 1 XRD pattern of the copper smelting slag before reduction

Table 1 Composition of copper slag by XRF and its *magnetite content

Fe	SiO$_2$	Al$_2$O$_3$	CaO	Zn	Cu	S	As	Pb	Ni	Co	Sb	*Fe$_3$O$_4$
39.47	30.72	5.07	1.41	1.91	0.67	0.55	0.42	0.18	0.08	0.06	0.04	10

Fig. 2 Schematic of the vertical furnace used for copper slag reduction experiments

a clean and sustainable reductant to replace the traditional reductants. Li et al. [25] experimented with waste cooking oil as a reductant to reduce iron in electric furnace copper smelting slag and the results indicated that after a reduction time of 4 min, the reduction efficiency of magnetic iron was over 90% and iron content in the slag was reduced to less than 2%. Holland et al. [26] investigated the reduction behavior of copper smelting slag flotation tailings below its melting point at 700–900 °C using methane and hydrogen as reductants. The study showed complete reduction of magnetite within the first 30 min of the process and the harmful impurities such as antimony, arsenic, bismuth, lead and zinc,

present as oxides in the slag were reduced and removed from the slag as flue dust in the process off-gas. Zhang et al. [27] conducted molten copper slag reduction with CO–H_2–Ar mixed gas as a reductant and reported that the reduction rate of CO and H_2 mixture was higher than that of pure CO or H_2. Zhou et al. [28] employed walnut shell pyrolyzed at 600 °C, while Kumar et al. [29] used macadamia nutshell pyrolyzed at 500–1300 °C as reductant in waste copper slag reduction for iron recovery. The studies revealed that biochars derived from pyrolyzed walnut shell and macadamia nutshell are effective, environmentally friendly reductants to reduce iron from waste copper slags and realize the cleaner utilization of

Table 2 The average detection limits for the metal and slag from EPMA, and for slag from LA-ICP-MS analysis in ppm

EPMA metal	Si	Co	Ni	As	Na	O	Al	Mg	Ca	K	S	Fe	Zn	Cu	Ti	Cr	Sb	Sn
	215	300	260	4247	427	1249	288	246	78	83	107	174	354	308	212	176	382	472
EPMA slag	Si	Co	Ni	As	Na	O	Al	Mg	Ca	K	S	Fe	Zn	Cu	Ti	Cr	Sb	Sn
	242	324	300	4925	619	580	385	224	90	95	124	203	414	409	221	189	406	540
LA-ICP-MS slag				^{29}Si					^{59}Co					^{60}Ni				^{75}As
				9.778					0.014					0.119				0.114

hazardous waste. Pyrolysis of biomass removes moisture and volatiles and increases the carbon content in biochar. This improves its reduction behavior, making biochar an ideal substitute for traditional reductants [30].

In this work, the reduction behavior of copper smelting slag with different biochars was studied in order to recover valuable elements such as copper and eliminate volatile impurities into gas phase. The study aims to also produce reusable slag which can be applied in other industries, such as road construction.

The kinetics of copper slag reduction were studied at different temperatures with several solid reductants. The concentrations of CO and CO_2 in the off-gas were monitored and the phase compositions of quenched samples were analyzed. Thermodynamic simulations were carried out with FactSage and HSC and compared with the experimental results.

Experimental

Materials Used

Industrial copper smelting slag was used for the experiments. The slag composition from XRF (X-ray fluorescence) analysis and magnetite concentration of the copper slag are shown in Table 1. Magnetite analysis was carried out using a Satmagan instrument (Outokumpu, Finland). The analysis revealed the iron content of 39.47 wt% and magnetite content of 10 wt%. X-ray diffraction (PANanalytical X'PERT PRO MPD Alpha 1) analysis was performed on the slag and is shown in Fig. 1. The main phases identified were fayalite, and magnetite.

Four (4) different kinds of reducing agents (L600, L1200, B600 and B1200), which were also used in our previous work for nickel slag reduction [31] were employed for reduction of the copper slag. The reductants consisted of lignin (L) and

black pellet (B), which were each pyrolyzed at 600 and 1200 °C. The proximate analysis showed that fixed carbon in lignin (L1200, 97.54 wt% and L600, 92.62 wt%) is higher than in black pellet (B1200, 83.19 wt% and B600, 76.16). Black pellet was shown to have higher ash content while volatile matter content was higher in biochar pyrolyzed at lower temperatures. The ultimate analysis also revealed that while biomass pyrolyzed at 1200 °C had virtually no hydrogen content, L600 and B600 contained nearly 2 wt% hydrogen. None of the biochars employed contained sulfur but had low concentrations of nitrogen [31].

The gases used in the high-temperature smelting experiments were purchased from Woikoski (Finland) and their purities were 99.999 vol% (N_2) and 99.999% (Ar). During the experiments, the samples were contained in silica glass crucibles (manufactured by Finnish Special Glass Oy, Espoo, Finland; material fused quartz; purity > 99.998%; outer diameter 25 mm, outer depth 15 mm).

Experimental Method

The experimental method used in this study is similar to that described in our previous study [31]. One gram of copper smelting slag was mixed with the calculated amount of each reductant in an agate mortar and the mixture was pelletized using a hydraulic press. The stoichiometric amount of carbon required for the reduction of the metal oxides (C/O) was calculated using Eqs. (1)–(6). Excess biochar was used (C/O ~ 2) during the reduction experiments.
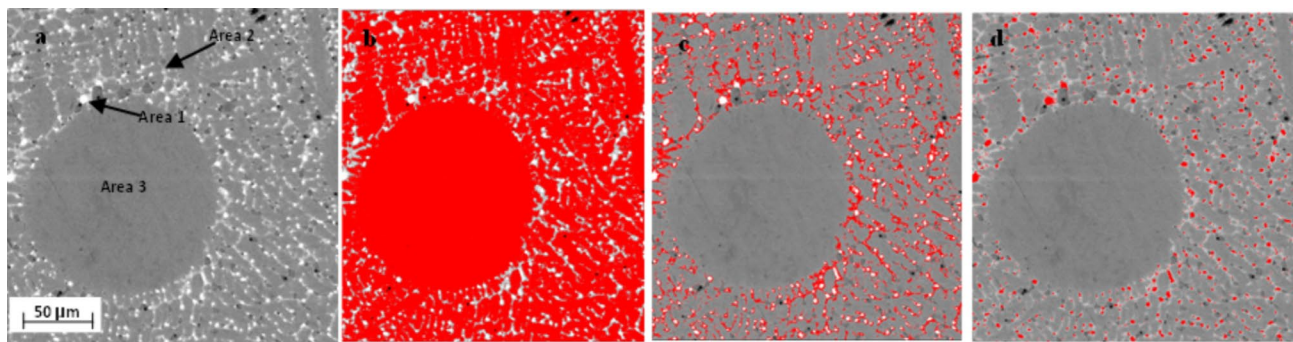
$$Fe_3O_4 + C = 3FeO + CO \tag{1}$$

$$NiO + C = Ni + CO \tag{2}$$

$$Cu_2O + C = 2Cu + CO \tag{3}$$

Fig. 3 Typical microstructure of the metal alloy from copper slag smelting showing **a** different areas visible, **b** image with adjusted thresholds for measuring the area percentage of Area 3 **c** image with adjusted thresholds for measuring the area percentage of Area 2, **d** image with adjusted thresholds for measuring the area percentage of Area 1
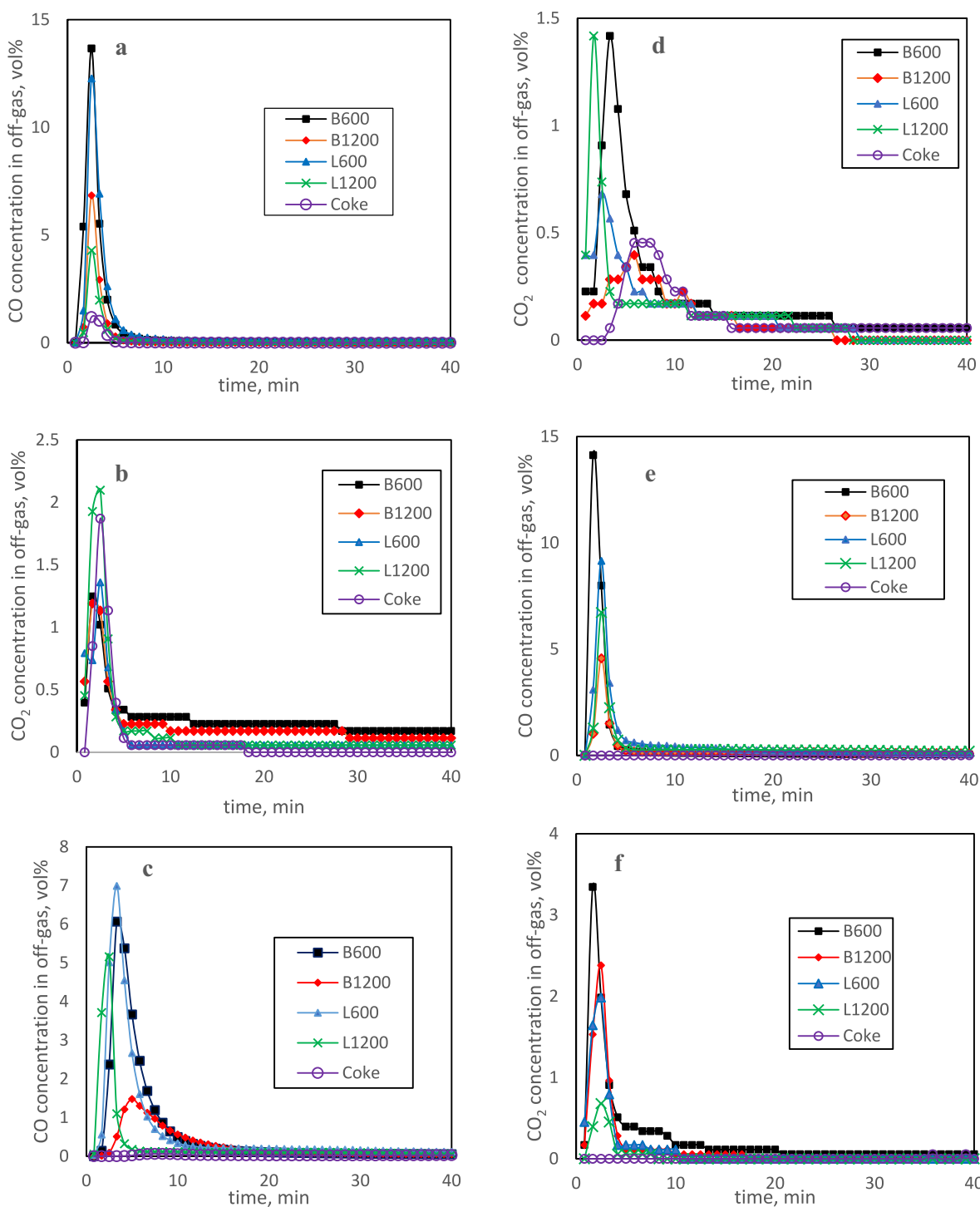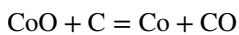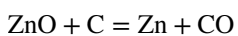
Fig. 4 Concentrations of **a** CO at 1250°C, **b** CO_2 at 1250°C, **c** CO at 1300°C, **d** CO_2 at 1300°C, **e** CO at 1350°C, and **f** CO_2 at 1350°C in the off-gas for 60 min during copper slag reduction with B600, B1200, L600, and L1200 biochar and metallurgical coke

$$ZnO + C = Zn + CO \tag{4}$$

$$CoO + C = Co + CO \tag{5}$$

$$\frac{1}{3}As_2O_3 + C = \frac{2}{3}As + CO \tag{6}$$

The pellet was placed in the crucible, which was in a basket shaped sample holder made from Kanthal A-wire

(diameter 0.5 mm). The reduction experiments were carried out in a vertical tube furnace (Lenton, UK) and purged with 300ml/min Ar gas, which has been described in our previous article. Figure 2 illustrates the experimental setup. The off-gases were analyzed using Gasmet FT-IR gas analyzer model DX4000, (Gasmet Technologies Oy, Vantaa, Finland) to measure the CO and CO_2 concentrations during the experiments. The flowrates of the input gasses were controlled by rotameters (R in Fig. 2) and the off-gas was

filtered (F in Fig. 2) to prevent dust from entering the gas analyzer. Nitrogen gas was flushed constantly into the gas analyzer with a flowrate of 1400 ml/min to obtain sufficient total gas flowrates for reliable gas analyzer operation (see Fig. 2). The additional nitrogen was introduced to the gas line after the furnace, so it did not enter the furnace and thus did not influence the reactions. The intervals in which the off-gas composition was measured were 50 s long (30 s of pumping gas to the chamber followed by 20 s of gas

Fig. 5 SEM micrographs of polished sections of copper slag reduction samples with **a** B600 for 60 min, **b** B600 for 30 min, **c** B600 for 15 min, **d** B1200 for 60 min, **e** B1200 for 30 min, **f** B1200 for 15 min, **g** L600 for 60 min, **h** L600 for 30 min, **i** L600 for 15 min, **j** L1200 for 60 min, **k** L1200 for 30 min, **l** L1200 for 15 min, **m** Coke for 60 min, **n** Coke for 30 min, and **o** Coke for 15 min at 1250 °C
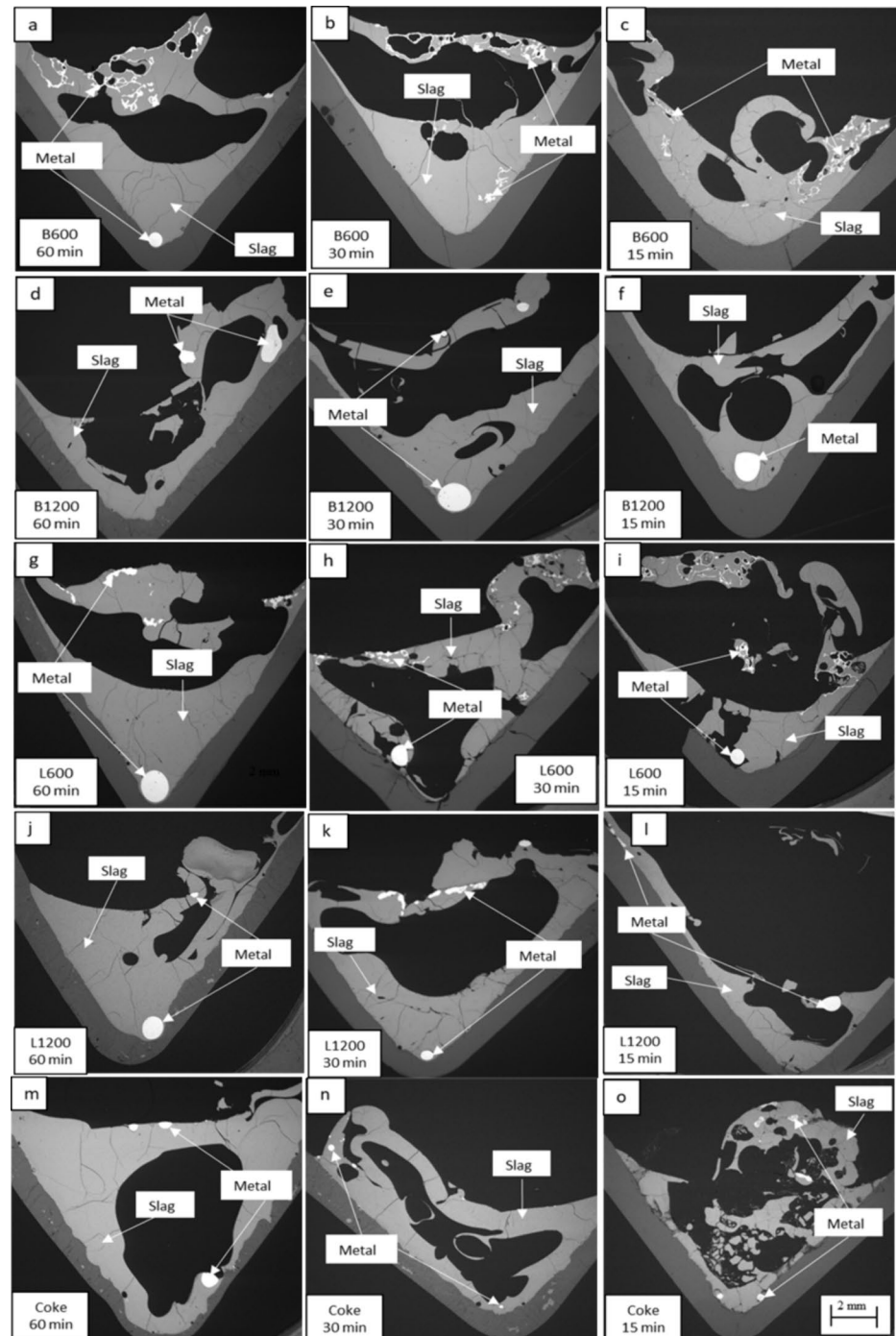
analysis). The experiments were carried out at 1250, 1300 and 1350 °C for 60 min to study the effect of temperature on reduction. Additionally, the effect of reaction time was studied at 1250 °C for 15, 30 and 60 min for each reductant.

Sample Characterization

At the end of each experiment, the samples were rapidly quenched in ice water, dried, and subsequently cast in epoxy. After curing, the samples were polished, and carbon coated for scanning electron microscopy (SEM) and electron probe microanalysis (EPMA). Mira 3 Scanning Electron Microscope (Tescan, Brno, Czech Republic) equipped with an UltraDry Silicon Drift Energy Dispersive X-ray Spectrometer (EDS) supplied by Thermo Fisher Scientific (Waltham, MA, USA) was used to perform preliminary elemental analyses and microstructural imaging.

The compositions of the metal and slag phases were quantified using EPMA with an SX100 (Cameca SAS, Gennevilliers, France) microprobe equipped with five wavelength dispersive spectrometers (WDS). Eight points were selected in the slag phase and twelve for the metal phase and the detection limits for the elements were determined separately in each analytical series. The accelerating voltage and beam current used were 20 kV and 30 nA, respectively. A defocused (5, 10 or 20 μm) electron beam was used. Standardization of the characteristic X-ray lines to be measured for the individual elements were carried out by using natural and synthetic minerals and metals as follows: Si Kα (quartz), O Kα (obsidian), Mg Kα and Ca Kα (diopside), Al Kα (almandine), Ni Kα (pure nickel), Co Kα (pure metal), Cr Kα (chromite), Ti Kα (rutile), Fe Kα (hematite), Cu Kα (pure copper), Zn Kα (sphalerite), S Kα (sphalerite), Na Kα (tugtupite), K Kα (sanidine), Sb Lα (SbTe), As Kβ (GaAs), and Sn Lα (pure metal). Totals of the individual analysis points obtained with EPMA were typically within 100 ± 2 wt%. The PAP–ZAF matrix correction by Cameca internal PeakSight analysis software was used for the primary WDS data [32]. The detection limits are presented in Table 2.

The concentrations of Ni, Co and As in the slags were below the detection limits of EPMA, therefore the slags were analyzed using laser ablation-inductively coupled plasma-mass spectrometry (LA-ICP-MS) comprising an ArF excimer laser (Teledyne CETAC Technologies, Omaha, USA) and a single-collector sector field ICP-MS (Nu Instruments Ltd., Wrexham, UK). The laser was fired at 10 Hz frequency with a 40 μm spot size. Eight spots were analyzed from each sample, and 40 s of time-resolved analysis signal was obtained from each spot. The signals were treated using Glitter-software [33]. USGS GSE-1G glass was used as the external standard, and ^{29}Si (from EPMA analysis) as the internal standard. USGS GSD-1G as well as BHVO-2G and
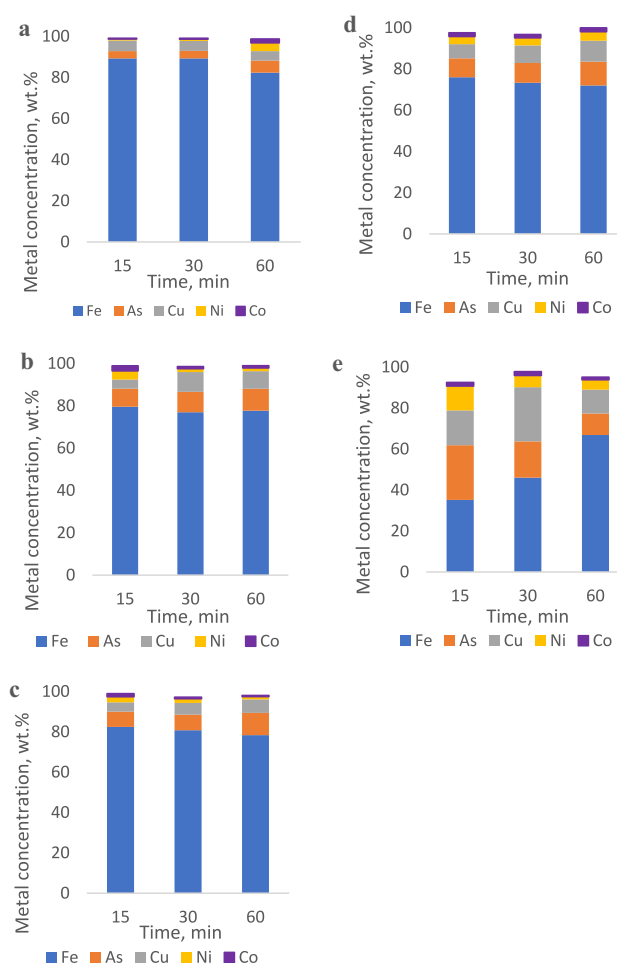

Fig. 6 Concentrations of iron, arsenic, copper, nickel, and cobalt in metal phase as a function of time during copper slag reduction with **a** B600, **b** B1200, **c** L600, and **d** L1200 biochars and **e** metallurgical coke at 1250 °C

BCR-2G glasses were analyzed as reference materials [34]. The obtained detection limits are shown in Table 2.

The metal alloy formed after reduction was found to be heterogenous. A typical microstructure of metal alloy is shown in Fig. 3a. Three different areas (Area 1 = white spots, Area 2 = light gray, Area 3 = gray) corresponding to different phases were identified. A statistical approach was used to calculate the average chemical composition. Several SEM images of the metal alloy were taken from each sample depending on the size of the metal alloy visible in the sample cross-section. The micrographs were taken with 1000 × magnification and the same brightness and contrast settings were used for all samples. Each image was then analyzed with ImageJ Fiji software, which allowed measuring the area percentage of each of the phases. The threshold of the image was adjusted in a way to select a desired area as shown in Fig. 3b, c, and d. After that, the average area percentage for each of the phase was calculated for each sample, based on

Fig. 7 Concentrations of **a** copper, **b** nickel, **c** arsenic, **d** iron and **e** cobalt in slag as a function of time during copper slag reduction with B600, B1200, L600, and L1200 biochars and metallurgical coke
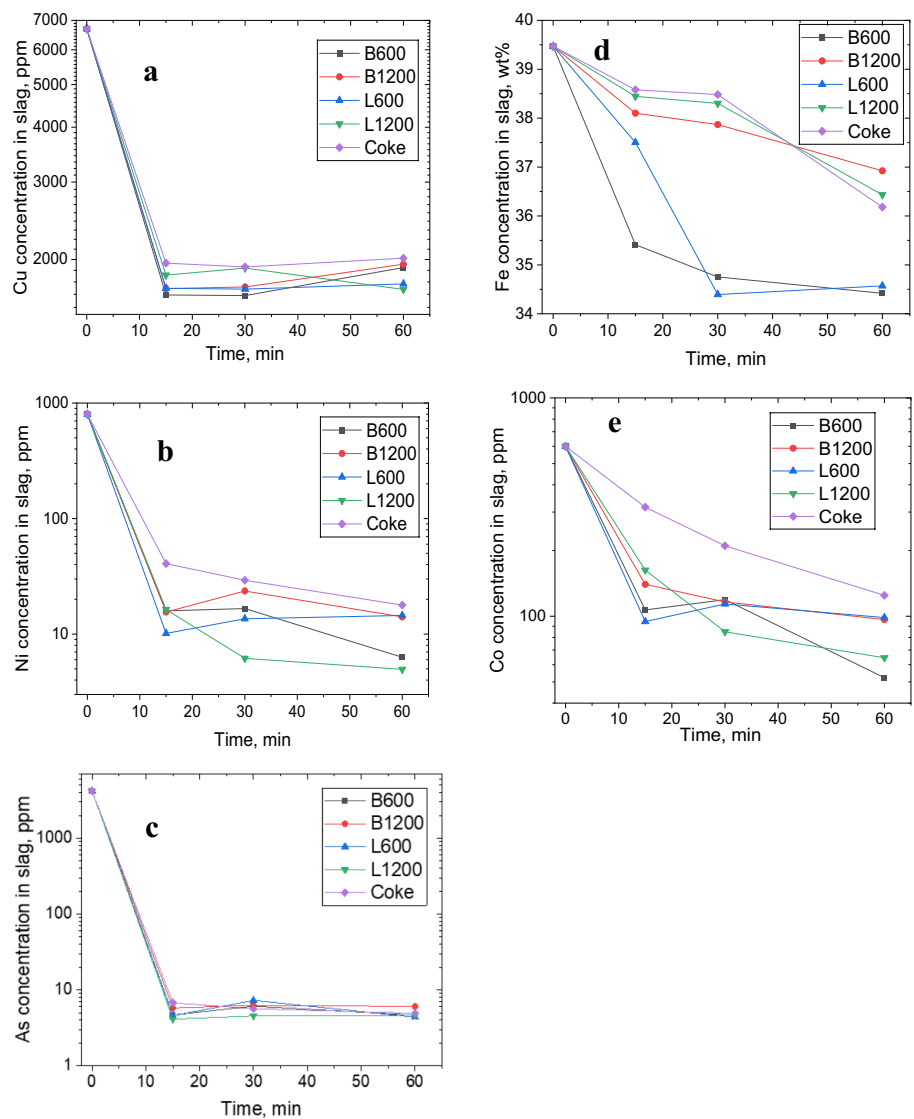
the SEM images obtained. The measured area fractions are equivalent to the volume fractions of each precipitate. The volume fraction of a precipitate can be converted to mass fraction of the precipitate by incorporating density of the precipitate and the overall density of the metal phase. However, it was assumed that the different areas of the metal phase have the same densities which makes it possible to multiply area percentage with weight percentage in Eq. (7). This assumption obviously introduces some uncertainty to the calculations. However, if the bulk metal density as well as densities of different areas would have been considered, assumptions would also have been needed.

After analyzing the compositions of each area (Area 1, Area 2 and Area 3) with EPMA, the average chemical concentration of each element in the metal alloy was calculated according to Eq. (7):

$$C_{Me(metalalloy)} = \frac{C_{Me(A1)}X_{(A1)} + C_{Me(A2)}X_{(A2)} + C_{Me(A3)}X_{(A3)}}{100}$$
(7)

where $C_{Me(metal\ alloy)}$ is the average concentration of metal Me in metal alloy (wt%); $C_{Me(A1)}$ is the average concentration of metal Me in Area 1 (wt%); $X_{(A1)}$ is the average weight percentage of Area 1; $C_{Me(A2)}$ is the average concentration of metal Me in Area 2 (wt%); $X_{(A2)}$ is the average weight percentage of Area 2; $C_{Me(A3)}$ is the average concentration of metal Me in Area 3 (wt%); $X_{(A3)}$ is the average weight percentage of Area 3.
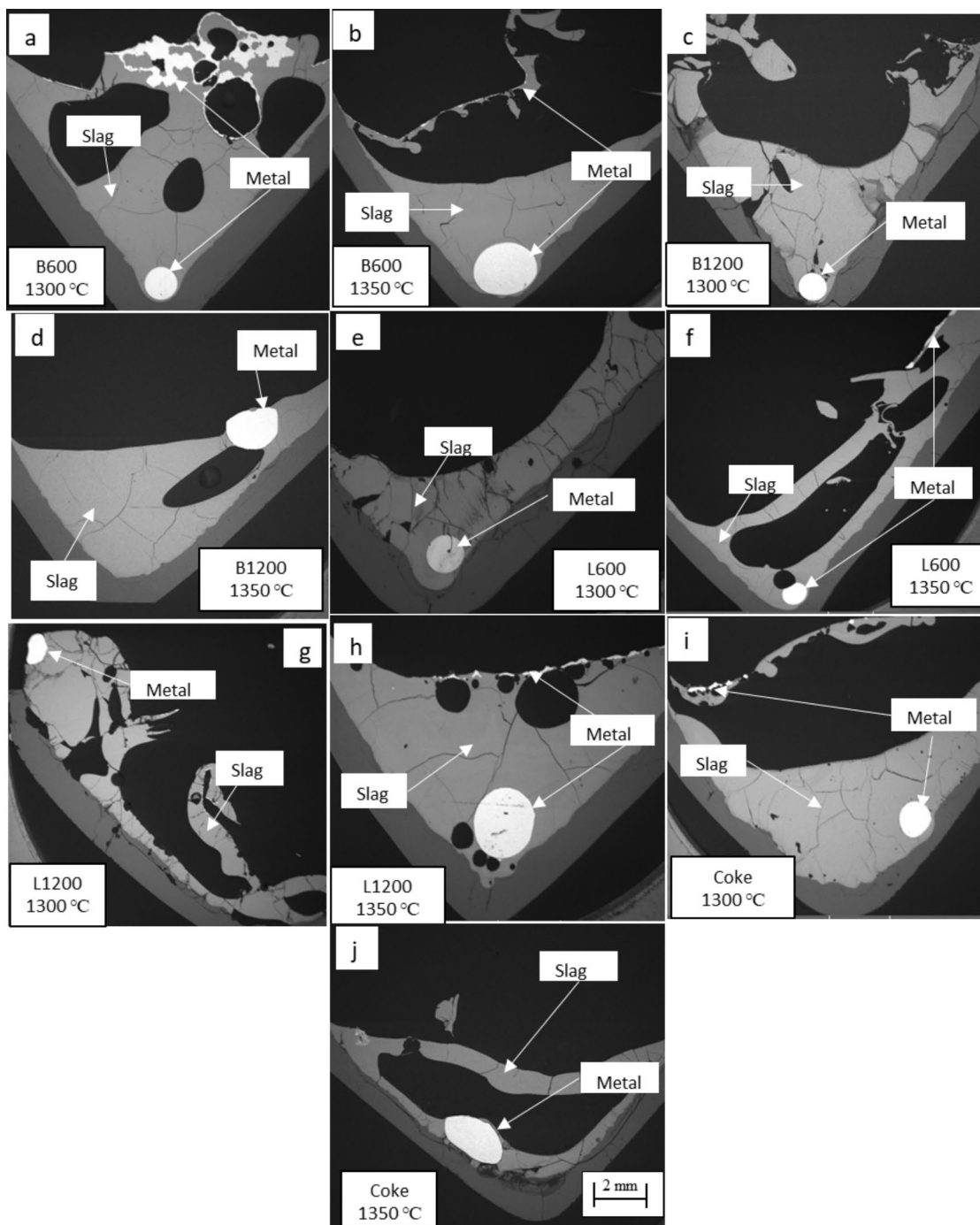
Fig. 8 SEM micrographs of polished sections of copper slag reduction with **a** B600 at 1300 °C, **b** B600 at 1350 °C, **c** B1200 at 1300 °C, **d** B1200 at 1350 °C, **e** L600 at 1300 °C, **f** L600 at 1350 °C, **g** L1200 at 1300 °C, **h** L1200 at 1350 °C, **i** Coke at 1300 °C, and **j** Coke at 1350 °C for 60 min

Results and Discussion

At the reduction temperatures, the carbon in biochar reacts with metal oxides present in the slag as seen in Eqs. (1)–(6).

It is reported that the degree of reduction of copper slag is enhanced at high temperatures and with sufficient time [35, 36]. The effect of reduction time and temperature have been investigated in this study.
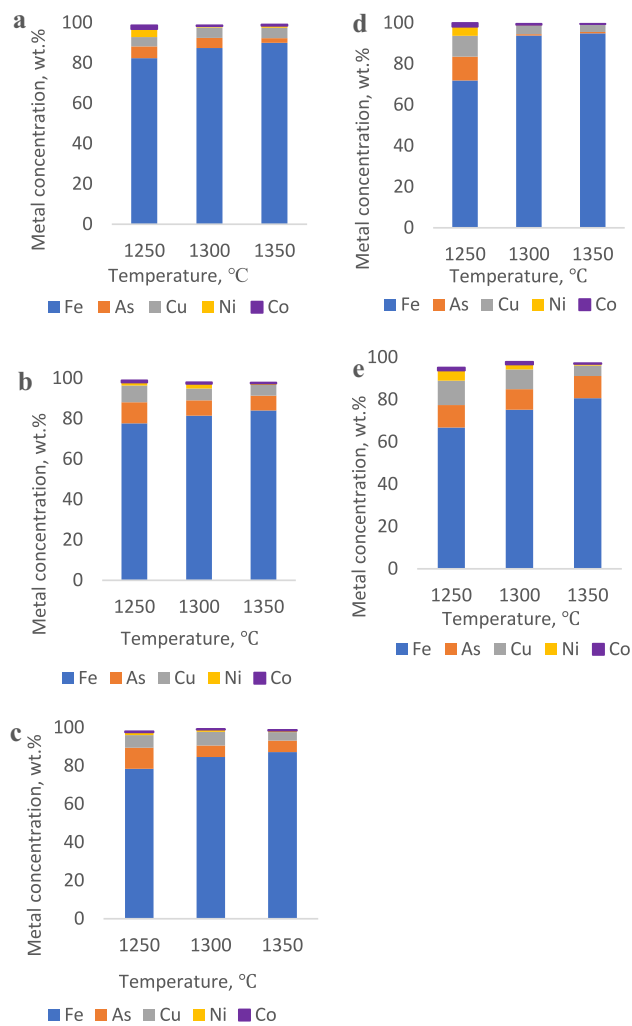
Fig. 9 Concentrations of iron, arsenic, copper, nickel, and cobalt in metal alloy as a function of temperature during copper slag reduction with **a** B600, **b** B1200, **c** L600, **d** L1200, and **e** coke for 60 min

Effect of Time on Reduction

The effect of reduction duration was studied at 1250 °C for 15, 30 and 60 min. The extent of reduction of metal oxides in the slag is expected to increase with time since more carbon and CO are expected to contribute to the reduction.

The concentrations of CO and CO_2 in the off-gas, during copper slag reduction with different reductants, are shown in Fig. 4. CO and CO_2 concentrations give an indication of the reduction rate and are related to the $p(O_2)$ during the reduction. Within 10 min of the reduction experiments, high amounts of CO and CO_2 were released, after which their concentrations decreased and remained close to zero until the end of the reduction experiments. The release of CO suggests the onset of reduction of copper slag. The

figure reveals that reduction occurs within the first 10 min. The reduction rate is highest within the first few minutes and as time progresses the metal phase is separated from the slag. Although the concentrations of CO and CO_2 in the off-gas may give an indication of how much oxygen is removed from the slag, in this case however, the presence of oxygen in the reducing agent (biochar) partially contributes to CO and CO_2 produced. The highest CO concentration in off-gas (14 vol%) was measured when B600 was used as reductant at 1250 °C. This may be ascribed to relatively high volatile matter content of the biochar, which makes it more reactive to the slag.

The SEM micrographs of the polished cross-sections are shown in Fig. 5. The samples completely melted even within 15 min at the hot zone.

The micrographs reveal that reduction has taken place to the extent that metal alloy droplets (bright area) were produced within the homogeneous slag. Generally, the metal alloy generated is present both at the top and at the bottom of the slag. Upon analyzing the sample, the metal alloy at the top was essentially iron (> 90 wt%) whereas the metal droplet at the bottom contained iron and significantly more other metals, particularly copper and arsenic.

This may be associated with settling differences. The copper and arsenic containing droplet settles to the bottom of the crucible along with the other metal elements. Part of the reduced iron present does not settle probably due to its high melting point. FactSage calculations reveal that, at the reduction temperature (1250 °C) both solid and liquid metal phases are stable. The solid metallic alloy phase, consisting predominantly of iron, remains at the top of the slag. Several studies have obtained similar micrographs where some metal alloy was found at the top edge of the slag and they reported that metallic iron firstly appears on the surface of the slag [37, 38]. In other studies on slag reduction [39–41], the authors found that the phase formed at the bottom of the slag contained sulfur (matte) while that present at the top was metal alloy. The two compositionally distinct metal alloys formed in this work may however be associated with the remnant of the matte dispersion in the original slag.

Moreover, it is as possible that this behavior may be attributed to surface and interfacial tensions between the phases of the system [39, 42]. The metal alloy has a high liquidus temperature and thus metal droplets may form mushy rafts that have difficulty settling through the slag layer.

The average concentrations of selected elements; iron, arsenic, copper, nickel, and cobalt in the metal alloy and slag are shown in Figs. 6 and 7, respectively. The concentrations of copper and arsenic in the metal increased slightly with time except in the reduction experiments with coke. HSC calculations show that copper and arsenic are the first metal elements to be reduced. Copper and arsenic combine

Fig. 10 Concentrations of **a** copper, **b** nickel, **c** arsenic, **d** iron and **e** cobalt in slag as a function of temperature during copper slag reduction with B600, B1200, L600, and L1200 biochar and metallurgical coke for 60 min
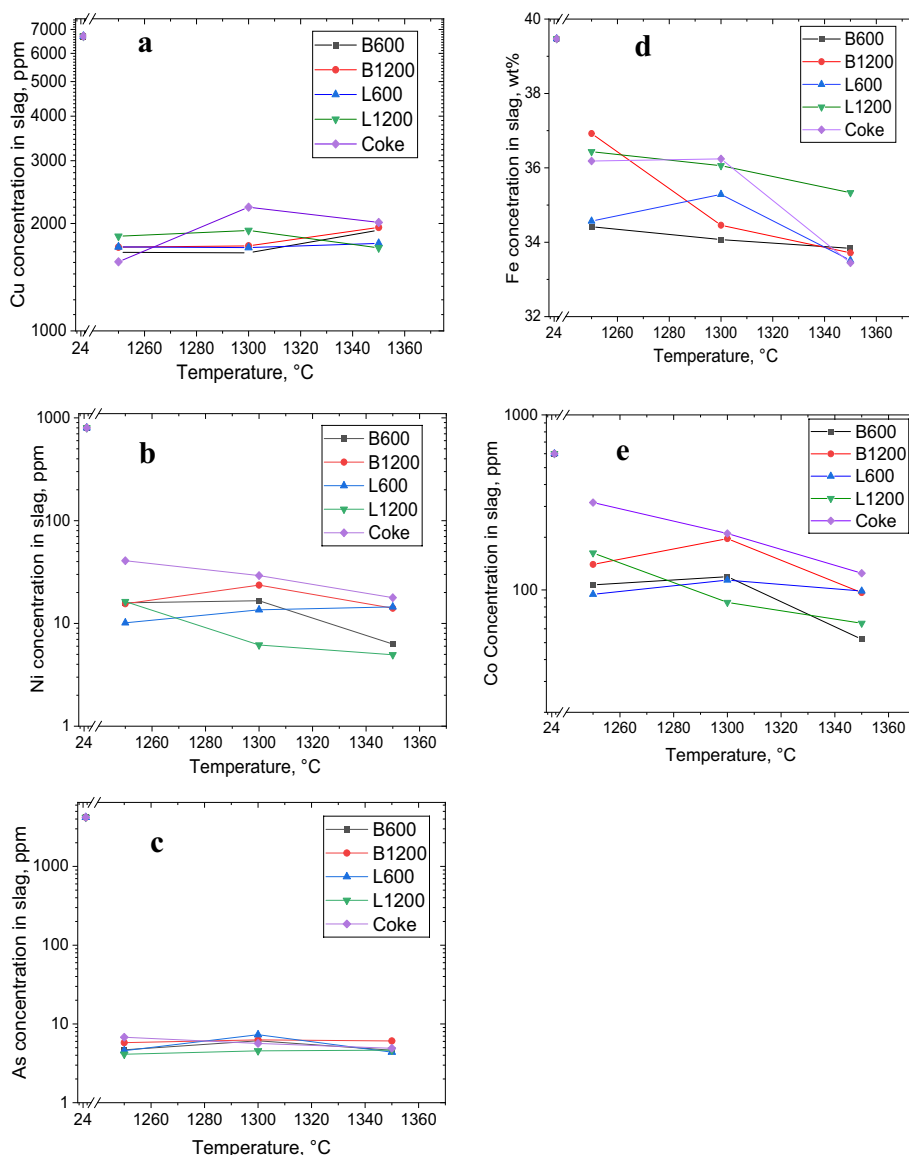
with other metal elements including nickel and iron and the metal droplet grows and settles to the bottom of the slag. As the amount of reductant used was twice the stoichiometric amount, significant part of iron oxide also reduced to metallic iron. After 60 min reduction, iron concentration in the metal was between 65 and 85 wt%.

Copper smelting slag reduction with B600 showed the highest iron concentration in the metal, but in general all biochar reductants showed greater reduction degrees of iron than coke. Several studies have indicated that biochar is more reactive and efficient than conventional reductants [43–45].

It is observed in Fig. 7 that within 15 min of reduction, the concentrations of copper, nickel and arsenic in the slag decreased dramatically (~90%). When coke was used as a reductant, cobalt concentration did not plummet as the

other metals, but rather decreased steadily as time progressed. The concentration of iron in the slag continuously decreased from 40 to 34 wt% when the most effective reductant, B600, was employed. It can be inferred from Fig. 7 that while increasing the reaction duration enhances the reduction of iron oxide from the slag, the removal of other metal elements, such as copper and arsenic, is not improved, which indicates that iron may be the 'last' element in the slag to be reduced into metal alloy. HSC simulations also reveal that iron is one of the last elements to be reduced by carbon at the studied temperatures. It should be noted that the concentrations of the metal elements in the slag at 0 min (Fig. 7) are the concentrations of the elements from the bulk analysis of original slag.
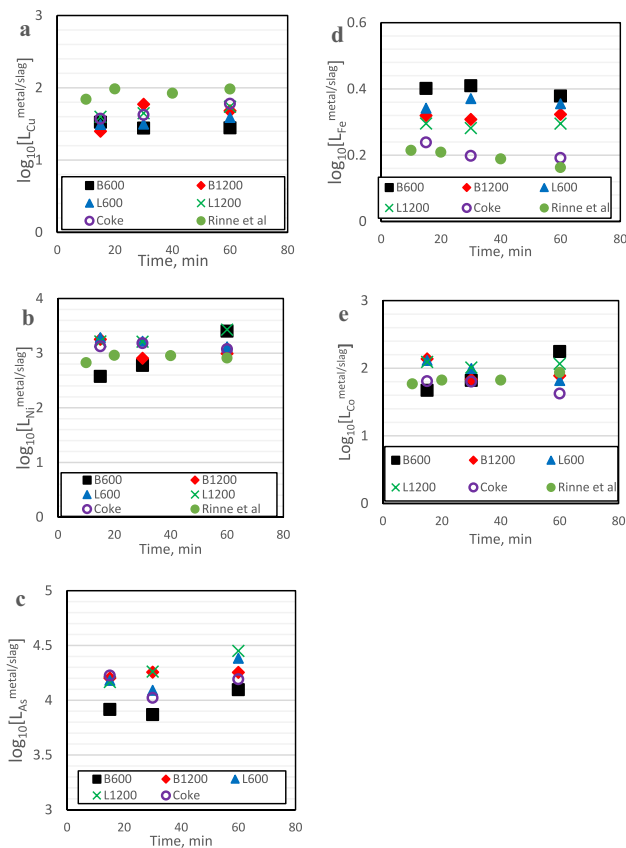
Fig. 11 Distribution coefficients of **a** copper, **b** nickel, **c** arsenic, and **d** iron, **e** cobalt between metal and slag as a function of time during copper slag reduction with B600, B1200, L600, and L1200 biochar and metallurgical coke at 1250 °C

Fig. 12 Distribution coefficients of **a** copper, **b** nickel, **c** arsenic, and **d** iron, **e** cobalt between metal and slag as a function of temperature during copper slag reduction with B600, B1200, L600, and L1200 biochar and metallurgical coke for 60 min

Effect of Reduction Temperature

The recovery of metals from copper slag using biochar was investigated at three different temperatures from 1250 to 1350 °C. Each experiment was carried out for 60 min. The samples were molten at the reduction temperatures and solidified after quenching. SEM micrographs of polished sections show that metal alloy was generated in each temperature. Metal recovery from slag is expected to increase with temperature since high temperatures can accelerate the diffusion and migration of metal atoms, which promotes the growth of metallic alloy particles. In the study, the amount of iron (solid metal phase) that was present on top of the slag decreased with increasing temperature (see Fig. 8). At higher temperatures, the slag is completely molten, and the reduced iron metal combined with the metal alloy droplet which settles at the bottom. This can be also seen in Fig. 8, as the size of the metal alloy droplet at the bottom of the crucible is generally larger at higher temperatures. It has been previously reported that a higher temperature promotes the Boudouard reaction (Eq. (8)), increases the CO concentration
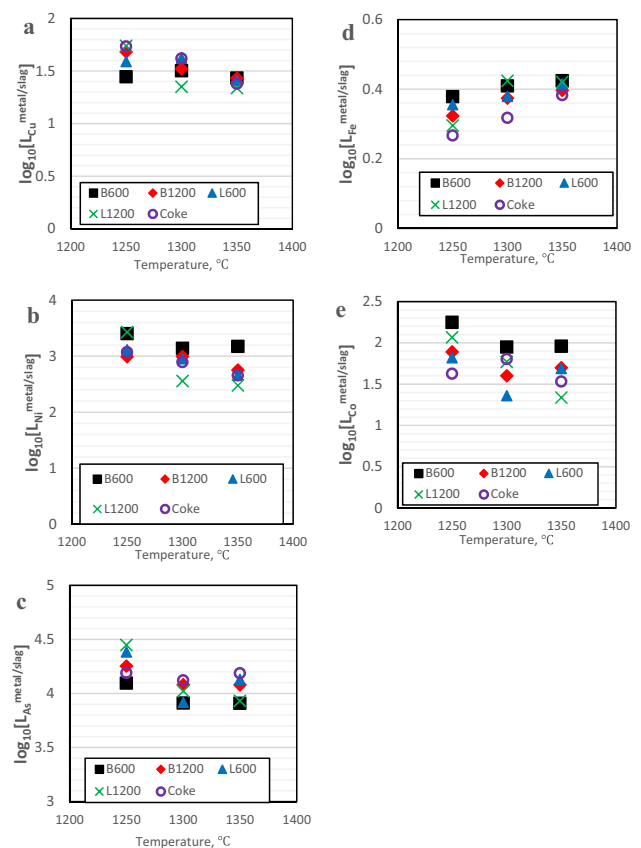
and enhances reduction process of metal-bearing minerals, which is beneficial for metallization degree of iron, copper, and nickel [46, 47].

$$C + CO_2 = 2CO \tag{8}$$

Figures 9 and 10 show the concentrations of Cu, Ni, As, Fe, and Co in the metal alloy and slag phases, respectively. Generally, the concentration of iron in the metal alloy increased with increasing temperature. The use of coke as reductant at 1250 °C resulted in the lowest iron concentration. This implies that while biochar is also effective at higher temperatures (> 1300 °C), at lower temperatures biochars are exceptionally more effective compared to coke.

At the reduction temperatures, the metal concentrations in slag were considerably lower compared to the starting material. Increase in temperature from 1250 to 1350 °C appears to have little effect on the removal efficiency of most of the metals from the slag. Although the iron concentration in slag decreases with increasing temperature, the change was

Fig. 13 Standard Gibbs energy of reactions that may take place during copper slag reduction from 700 to 1500 °C
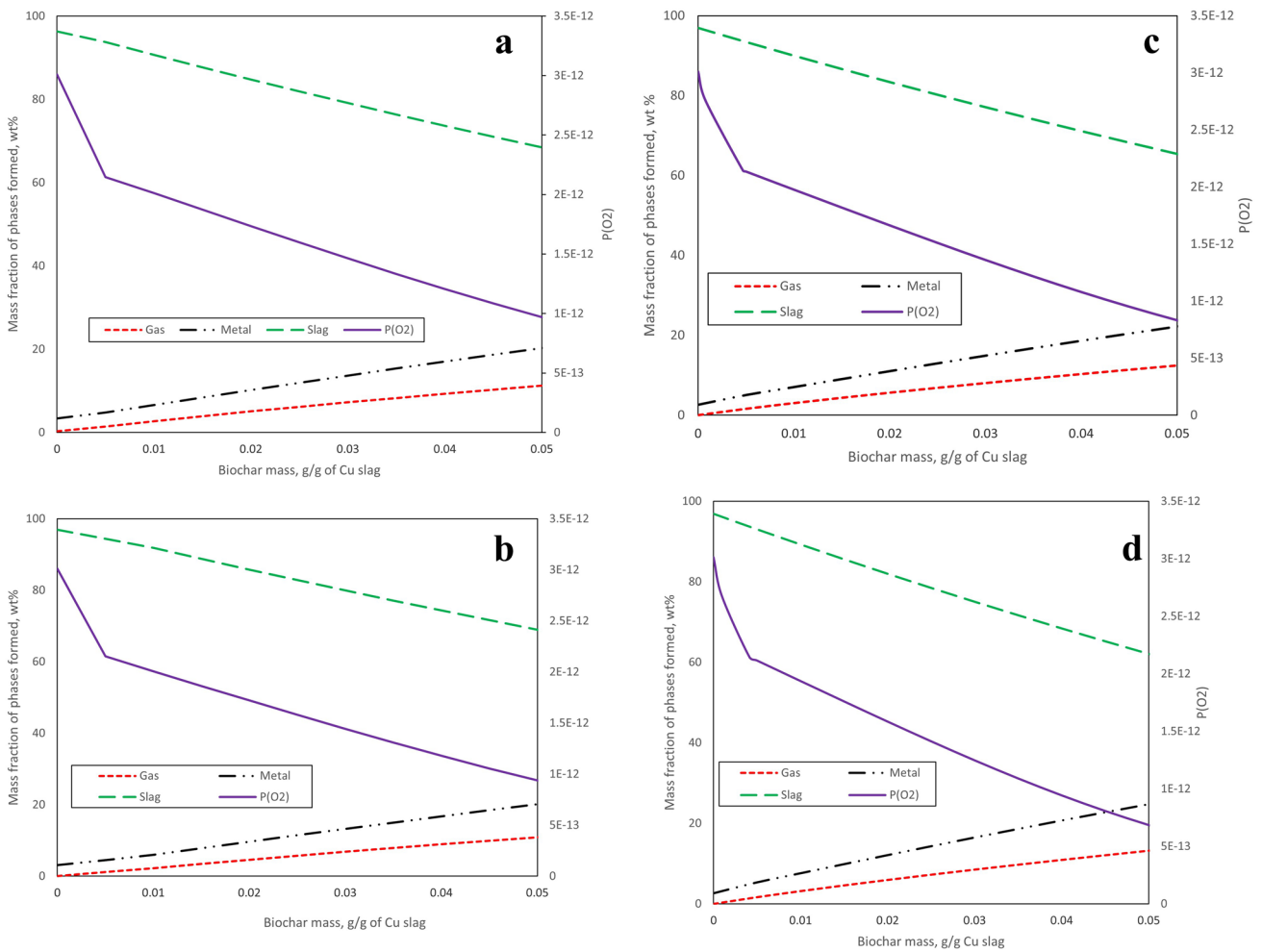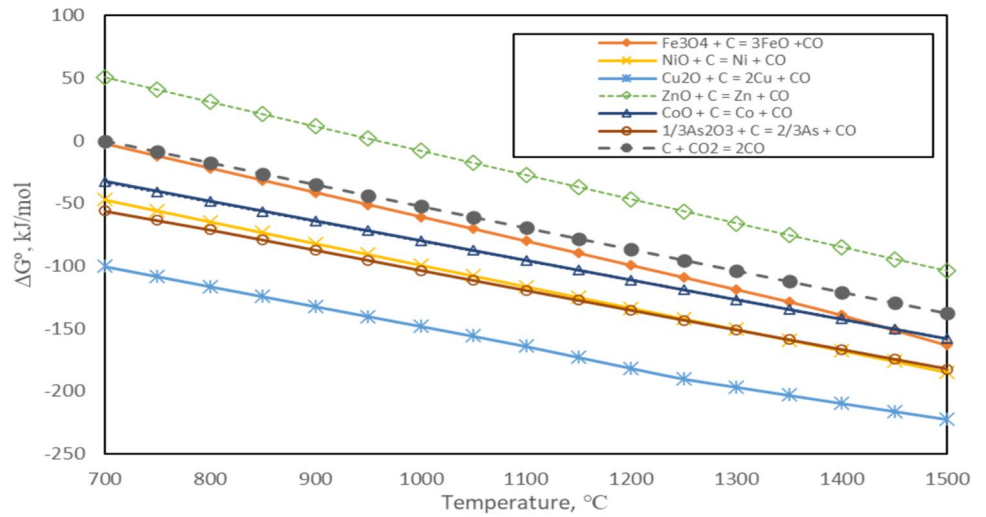
Fig. 14 Different phases formed during copper slag reduction with varying addition up to 0.05 g of **a** B600, **b** B1200, **c** L600, and **d** L1200 biochar per gram of copper smelting slag at 1250 °C as predicted by FactSage
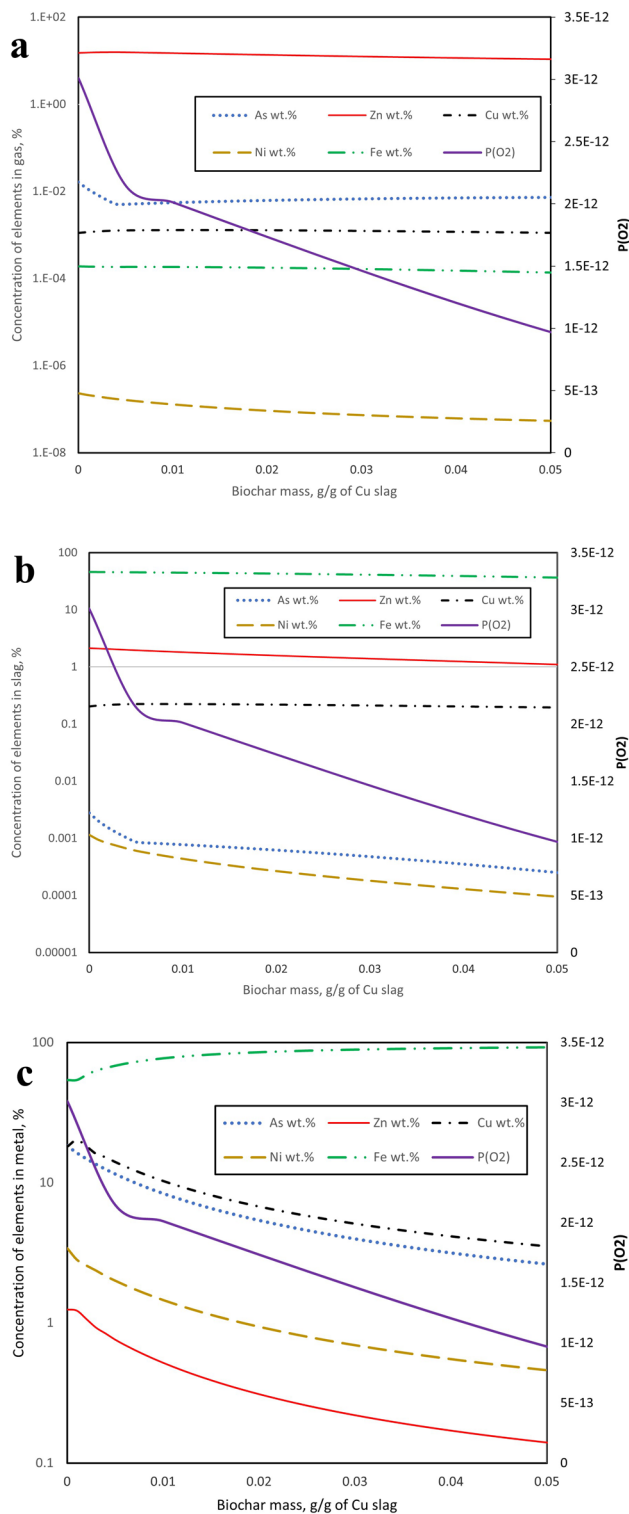
Fig. 15 Concentrations of arsenic, zinc, copper, nickel, and iron in **a** gas, **b** slag, and **c** metal phase during copper slag reduction with varying addition of B600 biochar to 1 g of copper slag as predicted by FactSage

not dramatic compared to the other metal species. The concentration of cobalt in slag on the other hand continuously decreased with the increase in temperature.

Distribution Coefficients of Elements During Experiments

Typically, the behavior of metals between different phases during high temperature reduction experiments is estimated using the metal to slag distribution coefficient. This value provides an indication of progress of the reaction kinetics and is related to the properties of the system and its species [39]. The distribution coefficient, L, of the element Me between metal and slag phases is expressed as the ratio of its weight concentrations in the metal alloy phase to slag phase (Eq. (9)).

$$L^m/s = \frac{wt\%Me\,in\,metal}{wt\%Me\,in\,slag} \tag{9}$$

Figure 11 shows the logarithm of the distribution coefficient of some elements between metal alloy and slag phases, as a function of time at 1250 °C. The calculated values were compared to those estimated from Rinne et al. [41] where metals recovered from the flotation fraction of industrial lithium-ion battery scrap were employed in high-temperature Cu-slag reduction at 1300 °C. It can be seen that results from this study are comparable to those of Rinne et al. The distribution coefficient for arsenic was the highest of all the metals of interest, while iron has the lowest coefficient. It is evident from Fig. 11 that increasing reduction time has the highest increasing effect on the distribution coefficients of Ni and As.

The distribution coefficients of copper, nickel, arsenic, iron, and cobalt after 60 min of reduction were also calculated as a function of temperature and are shown in Fig. 12. It is observed that generally, the distribution coefficient of iron increased as temperature increased while the values for other metals decreased with temperature. Arsenic and nickel distribution coefficients were the highest with the log values of the former between 4 and 5 and the latter between 2 and 4.

Thermodynamic Calculations

In this study, the reduction experiments were compared with thermodynamic simulations using the FactSage thermodynamic software package, version 8.0, and the HSC Chemistry software packages. HSC 10 was used to calculate the standard Gibbs energy to ascertain the reactions (see Eqs. (1)–(6) and (8)) that are feasible at the experimental temperatures and FactSage was used to investigate the effect of the addition of biochar on the composition of metal and slag. Copper slag composition (Table 1), as well

Fig. 16 Formation of gas, liquid metal, solid metal slag, spinel, and Fe_2SiO_4 phases during copper slag reduction of 1 g industrial copper slag with 0.02 g B600 biochar at different temperatures as predicted by FactSage
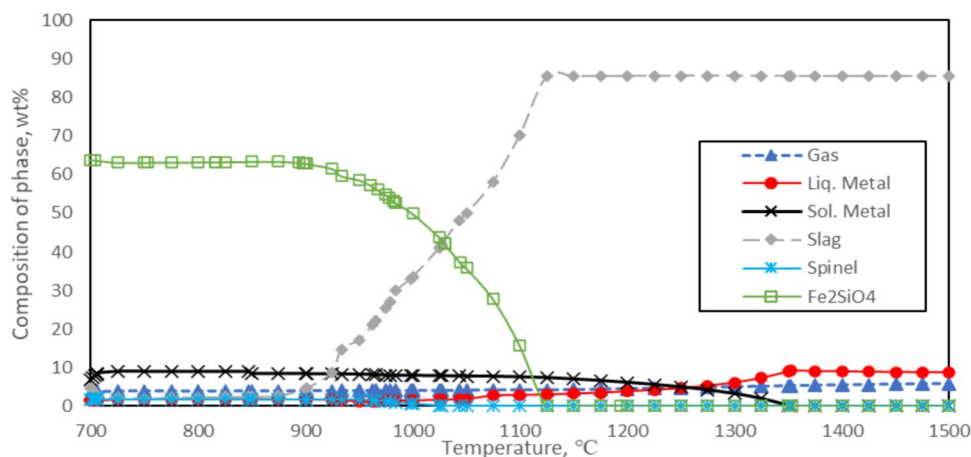
as the compositions of biochars [31] were used as inputs in FactSage . The databases used for the calculations were custom collected based on the databases FactPS (pure substances as well as gas phase), FToxid (optimized for oxide systems), and FSCopp (optimized for copper-containing solid and liquid alloys). The phases selected for the calculations were the spinel (solid solution phase with stoichiometry AB_2O_4, (A, B = divalent and trivalent metals), slag (liquid oxide silicate phase), monoxide phase (MeO solid solution), FCC, BCC, HCP-A3 (three solid multicomponent alloys of different crystallographic structures), and liquid metal. Ideal gas and pure solids were also selected before the calculations were done at the experimental temperature.

The standard Gibbs free energy ($\Delta G°$) of the reactions were determined from 700 to 1500 °C. Figure 13 shows that within the temperature range of the experiments (1250–1350 °C), the $\Delta G°$ values were less than zero, which indicates that the reactions with carbon are thermodynamically possible. In addition, the figure shows the sequence of reduction. The curves with the greatest negative values are the most likely to react initially. Copper oxide is first reduced followed by oxides of arsenic and nickel since they have the lowest Gibbs free energy at the experimental temperatures. It can be observed that iron and zinc oxides are the last to be reduced from the slag.

Effect of Biochar Addition

As predicted by FactSage , the phases formed during copper slag reduction at 1250 °C with biochar added to one gram of copper slag are shown in Fig. 14. It is seen that, for the different reductants, metal content as well as the gas amount increase as the mass of biochar increases, and the partial pressure of oxygen continues to decrease. This indicates that reduction degree rises with the addition of more biochar.

Reduction of copper smelting slag with B600 has been used to represent the other biochars as well, since similar

results were seen with the others. The concentrations of the main elements in the gas, slag and metal phases as well as the partial pressure of oxygen ($P(O_2)$) during reduction experiments are shown in Fig. 15. It is clearly shown that with the use of higher amount of biochar, reduction is increased which is illustrated by the decreasing $P(O_2)$. While zinc metal vaporised into the gas formed during the reduction, metal phase that formed had iron as the main component up to 90 wt%. The concentrations of elements generally decreased in the slag with higher biochar addition. Iron concentration in slag decreased to less than 35 wt% when 0.05 g of biochar was utilized as reductant for 1 g of copper slag. Copper and nickel concentrations also decreased in the slag with increasing biochar addition. Although the masses of the other metals in the metal alloy phase increase with biochar use, their weight percent concentrations were seen to decrease due to the higher extent of iron reduction. At the experimental conditions where approximately 0.02 g of biochar was added to 1 g one copper slag, the results from thermodynamic calculations with FactSage were consistent with the experimental results.

FactSage Predictions at Different Temperatures

The effect of temperature during copper slag reduction with biochar was investigated with FactSage , as shown in Fig. 16. FactSage predicts the presence of fayalite and spinel at lower temperatures (< 1200 °C). This validates the XRD analysis that shows the presence of fayalite and some spinel (Fe_3O_4) in the slag. At temperatures greater than 900 °C, liquid slag is produced and is predominant at 1150 °C and higher. The metal produced is present at liquid and solid forms during copper slag reduction. FactSage predicts that while liquid metal starts to form around 900 °C, the solid metal is absent only after 1350 °C. This confirms that the metal alloy found on top of the slag during the experiments
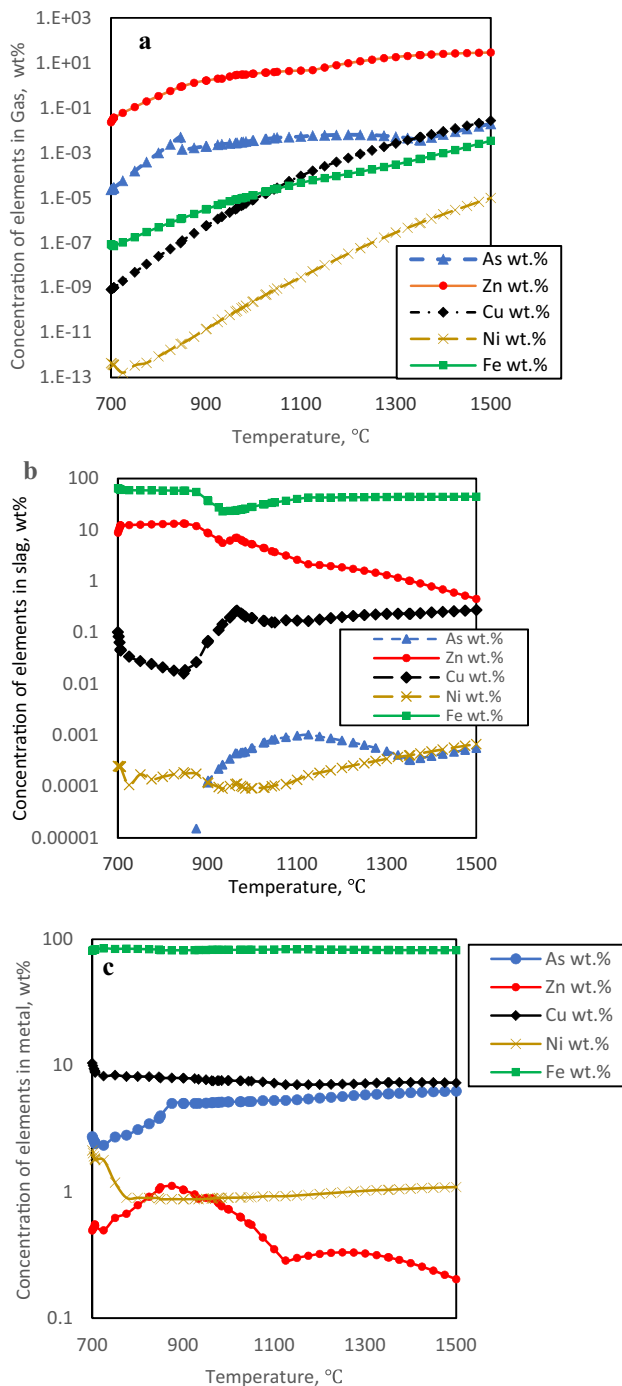
Fig. 17 Concentrations of arsenic, zinc, copper, nickel, and iron in **a** gas, **b** slag, and **c** metal alloy during copper slag reduction with B600 biochar at different temperatures as predicted by FactSage

is solid metal. The solid metal predicted by FactSage primarily consists of iron, which also supports the experimental findings.

In Fig. 17, the concentrations of the elements of interest in the gas, slag, and metal phase (consisting of both liquid and solid metal phase) produced during copper slag

reduction with biochar (B600) are shown as a function of temperature. Although the concentrations of most elements in the gas phase increase with increasing temperature, zinc has the highest percentage since it vaporizes at high temperatures. At 700 °C, zinc concentration in the gas phase is less than 1 wt%. It rises close to 30 wt% at 1500 °C, while the other metal elements have concentrations less than 0.1 wt%. In the slag and metal phases, FactSage predicts iron as the predominant metal element reaching up to 45 and 80 wt%, respectively, at 1500 °C. This is due to the high concentration of iron in the original slag. In the metal phase (total of liquid and solid metal), copper concentration decreased slightly from 10 to 7 wt% within the selected reduction temperature range.

Conclusions

The research conducted was aimed at determining the effectiveness of using biochar as reductant in pyrometallurgical cleaning of copper smelting slag. The effects of temperature, reduction duration and biochar type were studied. The results revealed that reduction using biochars is efficient and result in the formation of metal alloy.

Most of the reduction occurs within the first few minutes of the experiments due to the mixing and briquetting of slag and biochar, which were in powder form. As time progresses, the reduction continues at a lower rate. The reduced metals form a metal alloy droplet, which settles at the bottom of the crucible as time progresses, however solid metal particles were also present on top of the slag at lower reduction temperatures. Although with sufficient time reduction at 1250 °C is suitable, increasing temperature accelerates the diffusion and migration of metal atoms, promoting the growth of metallic alloy particles which then settle at the bottom of the crucible. While biochar is generally effective at all temperatures, it was found to be more efficient at lower temperatures compared to coke.

Volatile elements, such as zinc, vaporize to some extent during the smelting process and are transferred to the off-gas stream. During the reduction experiments, higher amounts of CO and CO_2 were released when biochar was applied as a reductant, compared to coke. Although the released CO gives an indication of the degree of oxygen removal, the presence of oxygen in the bio-reductants contributes to the amount of CO and CO_2 produced. HSC confirmed that at the experimental temperatures the reactions taking place are feasible and FactSage calculations agree well with the experimental results.

Declarations

Conflict of interest The authors declare that they have no conflict of interest.

References

1. Statista (2023) Copper mine production worldwide total 2022. Accessed 25 October 2023
2. Fan Y, Shibata E, Iizuka A, Nakamura T (2013) Review of iron recovery and cleaning of copper slag. J Min Mater ProcessInst Jpn 129:177–184. https://doi.org/10.2473/journalofmmij.129.177
3. Sarfo P, Das A, Wyss G, Young C (2017) Recovery of metal values from copper slag and reuse of residual secondary slag. Waste Manage 70:272–281. https://doi.org/10.1016/j.wasman.2017.09.024
4. Alp I, Deveci H, Süngün H (2008) Utilization of flotation wastes of copper slag as raw material in cement production. J Hazard Mater 159:390–395. https://doi.org/10.1016/j.jhazmat.2008.02.056
5. Gorai B, Jana RK, Premchand (2003) Characteristics and utilisation of copper slag—a review. Resour Conserv Recycl 39:299–313. https://doi.org/10.1016/S0921-3449(02)00171-4
6. Shi C, Meyer C, Behnood A (2008) Utilization of copper slag in cement and concrete. Resour Conserv Recycl 52:1115–1120. https://doi.org/10.1016/j.resconrec.2008.06.008
7. Potysz A, van Hullebusch ED, Kierczak J, Grybos M, Lens PNL, Guibaud G (2015) Copper metallurgical slags—current knowledge and fate: a review. Crit Rev Environ Sci Technol 45:2424–2488. https://doi.org/10.1080/10643389.2015.1046769
8. Rustandi A, Nawawi FW, Pratesa Y, Cahyadi A (2018) Evaluation of the suitability of tin slag in cementitious materials: mechanical properties and leaching behaviour. Mater Sci Eng 299:2–7. https://doi.org/10.1088/1757-899X/299/1/012046
9. Shanmuganathan P, Lakshmipathiraj P, Srikanth S, Nachiappan AL, Sumathy A (2008) Toxicity characterization and long-term stability studies on copper slag from the ISASMELT process. Resour Conserv Recycl 52:601–611. https://doi.org/10.1016/j.resconrec.2007.08.001
10. Banza AN, Gock E, Kongolo K (2002) Base metals recovery from copper smelter slag by oxidising leaching and solvent extraction. Hydrometallurgy 67:63–69. https://doi.org/10.1016/S0304-386X(02)00138-X
11. Busolic D, Parada F, Parra R, Sanchez M, Palacios J, Hino M (2013) Recovery of iron from copper flash smelting slags. Trans Inst Mining Metal C Mineral Process Extractive Metal 120:32–36. https://doi.org/10.1179/037195510X12772935654945
12. Bruckard WJ, Somerville M, Hao F (2004) The recovery of copper, by flotation, from calcium-ferrite-based slags made in continuous pilot plant smelting trials. Miner Eng 17:495–504. https://doi.org/10.1016/j.mineng.2003.12.004
13. Guo Z, Zhu D, Pan J, Wu T, Zhang F (2016) Improving beneficiation of copper and iron from copper slag by modifying the molten copper slag. Metals (Basel) 6:86. https://doi.org/10.3390/met6040086
14. Sarrafi A, Rahmati B, Hassani HR, Shirazi HHA (2004) Recovery of copper from reverberatory furnace slag by flotation. Miner Eng 17:457–459. https://doi.org/10.1016/j.mineng.2003.10.018
15. Anand S, Rao PK, Jena PK (1980) Recovery of metal values from copper converter and smelter slags by ferric chloride leaching. Hydrometallurgy 5:355–365. https://doi.org/10.1016/0304-386X(80)90025-0
16. Basir ASM, Rabah MA (1999) Hydrometallurgical recovery of metal values from brass melting slag. Hydrometallurgy 53:31–44. https://doi.org/10.1016/S0304-386X(99)00030-4
17. Herreros O, Quiroz R, Manzano E, Bou C, Viñals J (1998) Copper extraction from reverberatory and flash furnace slags by chlorine leaching. Hydrometallurgy 49:87–101. https://doi.org/10.1016/s0304-386x(98)00010-3
18. Shen H, Forssberg E (2003) An overview of recovery of metals from slags. Waste Manage 23:933–949. https://doi.org/10.1016/S0956-053X(02)00164-2
19. Ziyadanogullari B (2000) Recovery of copper and cobalt from concentrate and converter slag. Sep Sci Technol 35:1963–1971. https://doi.org/10.1081/SS-100100630
20. Heo JH, Kim BS, Park JH (2013) Effect of CaO addition on iron recovery from copper smelting slags by solid carbon. Metall Mater Trans B 44:1352–1363. https://doi.org/10.1007/s11663-013-9908-7
21. Kim BS, Jo SK, Shin D, Lee JC, Jeong SB (2013) A physicochemical separation process for upgrading iron from waste copper slag. Int J Miner Process 124:124–127. https://doi.org/10.1016/j.minpro.2013.05.009
22. Xian-Lin Z, De-Qing Z, Jian P, Teng-Jiao W (2015) Utilization of waste copper slag to produce directly reduced iron for weathering resistant steel. ISIJ Int 55:1347–1352. https://doi.org/10.2355/isijinternational.55.1347
23. Li KQ, Ping S, Wang HY, Ni W (2013) Recovery of iron from copper slag by deep reduction and magnetic beneficiation. Int J Miner Metall Mater 20:1035–1041. https://doi.org/10.1007/s12613-013-0831-3
24. Zhang L, Wu J, Yang H (2023) Study on thermal analysis kinetics of copper slag reduction. J Therm Anal Calorim 148:4267–4280. https://doi.org/10.1007/s10973-023-12038-y
25. Li B, Wang X, Wang H, Wei Y, Hu J (2017) Smelting reduction and kinetics analysis of magnetic iron in copper slag using waste cooking oil. Nat Sci Rep 7:1–9. https://doi.org/10.1038/s41598-017-02696-y
26. Holland K, Eriç RH, Taskinen P, Jokilaakso A (2019) Upgrading copper slag cleaning tailings for re-use. Miner Eng 133:35–42. https://doi.org/10.1016/j.mineng.2018.12.026
27. Zhang H, Bao L, Chen Y, Xuan W, Yuan Y (2021) Efficiency improvements of the CO-H₂ mixed gas utilization related to the molten copper slag reducing modification. Process Saf Environ Prot 146:292–299. https://doi.org/10.1016/j.psep.2020.09.011
28. Zhou S, Wei Y, Li B, Wang H (2019) Cleaner recycling of iron from waste copper slag by using walnut shell char as green

reductant. J Clean Prod 217:423–431. https://doi.org/10.1016/j.jclepro.2019.01.184

29. Kumar U, Maroufi S, Rajarao R, Mayyas M, Mansuri I, Joshi RK, Sahajwalla V (2017) Cleaner production of iron by using waste macadamia biomass as a carbon resource. J Clean Prod 158:218–224. https://doi.org/10.1016/j.jclepro.2017.04.115

30. Zhang B, Zhang T, Zheng C (2022) Reduction kinetics of copper slag by H_2. Minerals 548:2–14. https://doi.org/10.3390/min12050548

31. Attah-Kyei D, Sukhomlinov D, Tiljander M, Klemettinen L, Taskinen P, Jokilaakso A, Lindberg D, (2023) A crucial step toward carbon neutrality in pyrometallurgical reduction of nickel slag. J Sustain Metal, pp 1759–1776. https://doi.org/10.1007/s40831-023-00763-5

32. Pouchou J, Pichoir L (1986) Basic expression of "PAP" computation for quantitative EPMA. In: Proceedings of the 11th international congress on X-ray optics and microanalysis (ICXOM), London, ON, Canada, pp 249–256.

33. Van Achterberg E, Ryan CG, Jackson SE, Griffin WL (2001) Data reduction software for LA-ICP-MS: Appendix. Laser ablation-ICP-mass spectrometry in the earth sciences: principles and applications. Mineralogical Association of Canada, Ottawa, pp 239–243

34. Jochum KP, Willbold M, Raczek I, Stoll B, Herwig K (2005) Chemical characterisation of the USGS reference glasses GSA-1G, GSC-1G, GSD-1G, GSE-1G, BCR-2G, BHVO-2G and BIR-1G Using EPMA, ID-TIMS, ID-ICP-MS and LA-ICP-MS. Geostand Geoanal Res 29:285–302

35. Zhang L, Zhu Y, Yin W, Guo B, Rao F, Ku J (2020) Isothermal coal-based reduction kinetics of fayalite in copper slag. ACS Omega 5:8605–8612. https://doi.org/10.1021/acsomega.9b04497

36. Zuo Z, Yu Q, Wei M, Xie H, Duan W, Wang K, Qin Q (2016) Thermogravimetric study of the reduction of copper slag by biomass: reduction characteristics and kinetics. J Therm Anal Calorim 126:481–491. https://doi.org/10.1007/s10973-016-5570-z

37. Busolic D, Parada F, Parra R, Sanchez M, Palacios J, Hino M (2011) Recovery of iron from copper flash smelting slags. Trans Inst Mining Metal C Mineral Process Extractive Metal 120:32–36. https://doi.org/10.1179/037195510X12772935654945

38. Palacios J, Sánchez M (2011) Wastes as resources: Update on recovery of valuable metals from copper slags. Trans Inst Mining Metal C Mineral Process Extractive Metal 120:218–223. https://doi.org/10.1179/1743285511Y.0000000020

39. Avarmaa K, Järvenpää M, Klemettinen L, Marjakoski M, Taskinen P, Lindberg D, Jokilaakso A (2020) Battery scrap and biochar utilization for improved metal recoveries in nickel slag cleaning conditions. Batteries 6:3–21. https://doi.org/10.3390/batteries6040058

40. Dańczak A, Ruismäki R, Rinne T, Klemettinen L, O'brien H, Taskinen P, Jokilaakso A, Serna-guerrero R (2021) Worth from waste: utilizing a graphite-rich fraction from spent lithium-ion batteries as alternative reductant in nickel slag cleaning. Minerals 11:4–23. https://doi.org/10.3390/min11070784

41. Rinne T, Klemettinen A, Klemettinen L, Ruismäki R, O'brien H, Jokilaakso A, Serna-Guerrero R (2022) Recovering value from end-of-life batteries by integrating froth flotation and pyrometallurgical copper-slag cleaning. Metals (Basel) 12:2–24. https://doi.org/10.3390/met12010015

42. Matusewicz R, Mounsey E (1998) Using ausmelt technology for the recovery of cobalt from smelter slags. JOM 50:53–56. https://doi.org/10.1007/s11837-998-0355-x

43. Bagatini MC, Kan T, Evans TJ, Strezov V (2021) Iron ore reduction by biomass volatiles. J Sustain Metal 7:215–226. https://doi.org/10.1007/s40831-021-00337-3

44. Du J, Zhang F, Hu J, Yang S, Liu H, Wang H (2022) Direct reduction of copper slag using rubber seed oil as a reductant: Iron recycling and thermokinetics. J Clean Prod 363:1–13. https://doi.org/10.1016/j.jclepro.2022.132546

45. Huang D, Zong Y, Wei R, Gao W, Liu X (2016) Direct reduction of high-phosphorus oolitic hematite ore based on biomass pyrolysis. J Iron Steel Res Int, pp 874–883. https://doi.org/10.1016/S1006-706X(16)30134-0

46. Chen D, Guo H, Xu J, Lv Y, Xu Z, Huo H (2017) Recovery of iron from pyrite cinder containing non-ferrous metals using high-temperature chloridizing-reduction-magnetic separation. Metall Mater Trans B 48:933–942. https://doi.org/10.1007/s11663-017-0913-0

47. Gao C, Yu W, Zhu Y, Wang M, Tang Z, Du L, Hu M, Fang L, Xiao X (2021) Preparation of porous silicate supported micro-nano zerovalent iron from copper slag and used as persulfate activator for removing organic contaminants. Sci Total Environ 754:3–8. https://doi.org/10.1016/j.scitotenv.2020.142131